引用格式：JIN Yanping, LU Chunhui, ZHAO Qiyi, et al. Thickness-dependent Third-order Nonlinear Optical Absorption of WS_2 Nanofilms[J]. Acta Photonica Sinica, 2022, 51(4):0416002
靳延平,卢春辉,赵奇一,等. WS_2纳米薄膜厚度依赖的三阶非线性吸收特性研究[J].光子学报,2022,51(4):0416002

WS_2纳米薄膜厚度依赖的三阶非线性吸收特性研究

靳延平[1],卢春辉[1],赵奇一[2],徐新龙[1]
(1 西北大学 物理学院 光子学与光子技术研究所,西安 710069)
(2 西安邮电大学 理学院,西安 710121)

摘　要:利用液相剥离法制备了WS_2纳米片,结合真空抽滤技术,控制上清液体积制备了不同厚度的WS_2薄膜。在此基础上,使用800 nm飞秒激光的Z扫描技术表征了WS_2纳米薄膜的三阶非线性吸收特性。研究发现,制备的不同厚度的WS_2都表现出可饱和吸收特性,可饱和吸收主要是由于单光子吸收所引起的泡利阻塞效应引起;随着厚度的增加,饱和强度基本不变,调制深度会有所提高,但是三阶非线性极化率虚部的绝对值和品质因子会降低。这主要是因为较厚的薄膜缺陷更多,更容易捕获光生载流子,从而三阶非线性吸收和厚度有一定的依赖关系。可饱和吸收可以用于调Q激光器以及锁模激光器,为WS_2薄膜在超快开关和超快激光的应用提供实验支持。

关键词:二硫化钨;三阶非线性;可饱和吸收;厚度依赖;Z扫描
中图分类号:O437　　**文献标识码**:A　　**doi**:10.3788/gzxb20225104.0416002

0　引言

与传统的块体半导体材料不同,二维过渡金属硫族化合物作为一种新型的半导体材料,表现出优异的光学和电学特性,例如超快载流子动力学,长的载流子寿命,高的电子迁移率[1]。因其优异的光电特性,二维过渡金属硫族化合物已经成功应用在光电器件领域,例如光电探测器[2],发光二极管[3],场效应管[4],太赫兹宽带发射器件等[5-6]。作为典型的过渡金属硫族化合物,单层WS_2为直接带隙半导体(带隙~2 eV),块体则为间接带隙半导体(带隙~1.1 eV)[7]。这种带隙随层数可调的特性使得WS_2在强光作用下表现出很多新颖的非线性吸收特性[8],例如饱和吸收,反饱和吸收和双光子吸收等,为设计光限幅器件和锁模器件等光子学器件提供了实验和理论方面的支撑。

2015年DONG Ningning等[9]利用532 nm纳秒激光研究了入射光强对WS_2纳米片分散液的非线性吸收的影响,结果显示WS_2纳米片在较低的泵浦光强下表现出饱和吸收特性,然而随着泵浦能量的增加转变为反饱和吸收。该转变主要与热诱导的溶剂气泡引起的非线性光散射有关。同样在2015年ZHOU Kaige等[10]通过控制离心速度实现了不同尺寸的纳米片的有效分离,在532 nm皮秒激光激发下,小尺寸WS_2纳米片表现为反饱和吸收现象,然而大尺寸的纳米片表现为饱和吸收现象,这种尺寸依赖的非线性吸收特性主要源自边缘缺陷增强了激发态的吸收。2020年,LU Chunhui等为了研究尺寸对缺陷的影响,利用800 nm飞秒激光照射WS_2纳米片分散液,观察到随着纳米片尺寸的减小,非线性吸收特性出现从饱和吸收到反饱和吸收的转变,证实了小尺寸表面更容易发生氧化,从而增强双光子吸收[11]。然而,目前关于WS_2非线性吸收的研究大部分是在溶液环境下实现测量的,很容易引起热诱导的非线性散射并阻碍了非线性固体光子器件的应用。因此,从实际应用的角度来看,研究大面积纳米薄膜材料的非线性吸收特性变得尤为重要。

本文利用液相剥离技术制备了大尺寸的WS_2纳米片分散液,通过控制抽滤体积实现了大面积不同厚度的WS_2薄膜的制备。借助原子力显微镜表征平台,测得制备的WS_2纳米片约为3~4 nm,薄膜厚度最小可达

基金项目:国家自然科学基金(Nos.11774288, 12074311),陕西省自然科学基金(No. 2019-JC25)
第一作者:靳延平(1979-),女,工程师,硕士,主要研究方向为非线性光学,超材料设计。Email:yanpinghappy@nwu.edu.cn
通讯作者:徐新龙(1976-),男,教授,博士,主要研究方向为超快光学、非线性光学、太赫兹物理。Email:xlxuphy@nwu.edu.cn
收稿日期:2021-11-04;**录用日期**:2021-12-29

50 nm。利用自主搭建的开口Z扫描系统研究了WS_2薄膜厚度依赖的三阶非线性吸收特性。

1 实验

1.1 WS_2薄膜制备

实验采用液相剥离的方法制备WS_2纳米片，结合真空抽滤技术将获得的少层纳米片均匀堆叠在一起获得WS_2薄膜[12-13]。通过控制上清液的体积获得不同厚度的WS_2薄膜。合成过程为：称取300 mg的WS_2粉末分散在300 mL的50%异丙醇溶液中，超声破碎仪(Qsonica Q700)在75 W下工作1 h，产生的超声波诱使液体产生气泡，气泡破裂后会产生密集的张力破坏了二维材料层与层之间的范德瓦尔斯力，从而实现块体WS_2的剥离，最终得到不同层数的纳米片分散液。为了避免长时间破碎产生的热量在WS_2纳米片表面发生氧化，在恒温水浴中完成该过程。为了获得单层或少层纳米片，使用高速离心机(Centurion Scientifc K241)，设置的离心速度为7 000 r/min，成功实现了较厚的纳米片的分离，将获取的上清液静置两天后使用。控制上清液体积(30，40，50，60，70 mL)，进行真空抽滤得到几十至百纳米厚度的薄膜，最后在室温下将薄膜晾干。利用丙酮溶解掉滤膜，将WS_2薄膜样品转移到目标基底载玻片上。

1.2 Z扫描实验装置

实验中利用自主搭建的开口Z扫描技术提取WS_2的非线性吸收参数[14]。利用钛宝石激光器(Spectra-Physics Spitfre，800 nm，35 fs，1 000 Hz)作为入射光源。聚焦透镜的焦距为175 mm，会聚成束腰半径为35 μm的高斯光束，通过衰减片调节入射光泵浦能量，利用步进电动平移台实现样品在焦点附近移动，利用硅探测器(Thorlabs-PDA100A(-EC))接收透射的光信号。

2 结果与讨论

使用原子力显微镜(Atomic Force Microscopy，AFM)测量制备的WS_2纳米片的厚度，如图1(a)所示，结果

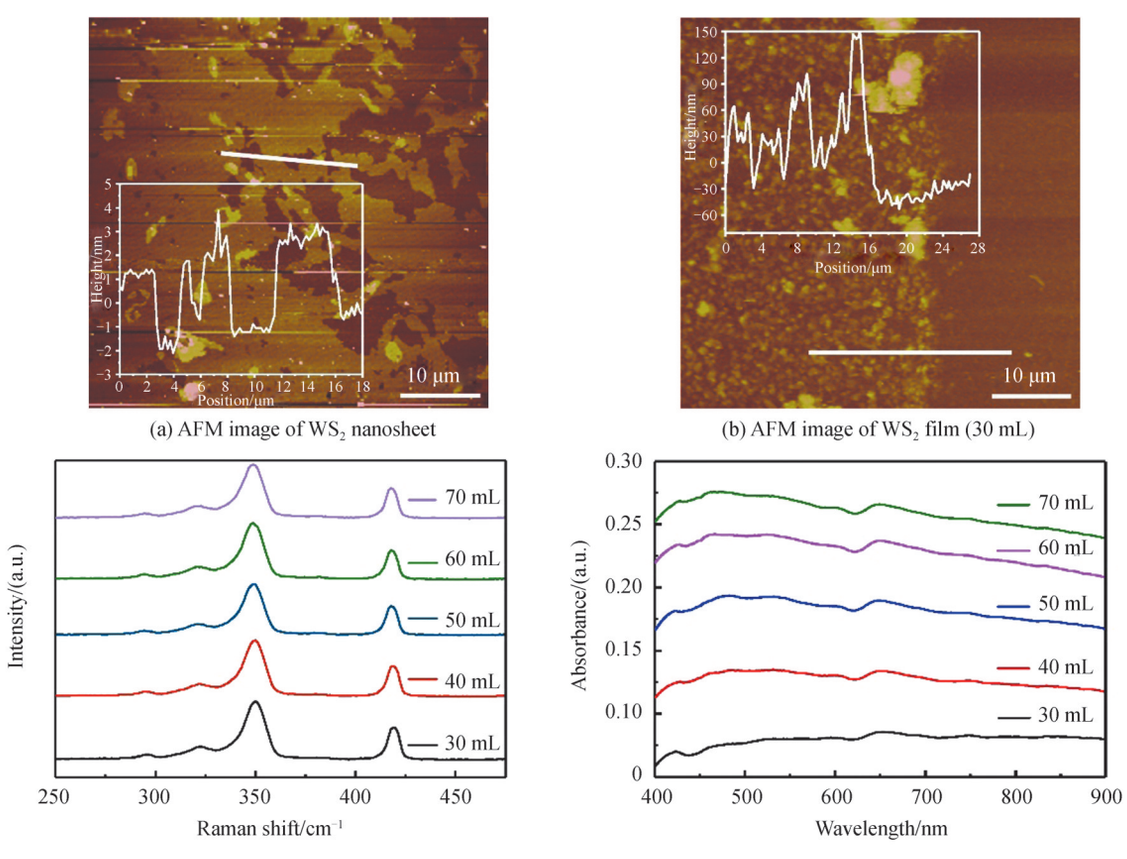

(a) AFM image of WS_2 nanosheet

(b) AFM image of WS_2 film (30 mL)

(c) Raman spectra of different thickness WS_2 films

(d) UV-vis spectra of WS_2 films

图1 制备的WS_2样品的表征

Fig. 1 Characterization of prepared WS_2 samples

显示纳米片厚度为3～4 nm约4～5层（单层～0.75 nm），单一纳米片的横向尺寸在2～4 μm范围内。如图1(b)所示，测量了抽滤30 mL的薄膜的厚度约为50 nm，抽滤体积为70 mL的薄膜厚度为130 nm，这种纳米片的堆叠更容易在晶界处产生缺陷。测量了不同厚度的WS_2纳米薄膜的拉曼光谱（激发波长为532 nm），如图1(c)所示。不同厚度的WS_2纳米薄膜中均观察到E^1_{2g}(348.76 cm^{-1})和A_{1g}(～418.84 cm^{-1})的晶格振动模式，证实了目标薄膜样品被成功制备。使用紫外-可见吸收光谱表征不同厚度的的WS_2薄膜的线性吸收特性(400～900 nm)，随着厚度增加出现明显的乌尔巴赫(Urbach)带尾，这与局域化的缺陷态增加有关，如图1(d)所示。

使用800 nm飞秒激光作为入射光源，以载玻片基底作为空白对照，研究发现在泵浦能量为700 nJ下并未观察到基底非线性吸收效应，可以排除基底对样品非线性吸收的干扰。图2(a)～(e)为不同厚度(30，40，50，60，70 mL)的WS_2薄膜随泵浦能量的Z扫描实验结果。研究发现随着入射光的能量增强其透射率也不断增加，即为典型的饱和吸收现象。这种饱和吸收是由于激发光子能量(1.55 eV)高于材料带隙引起的单光

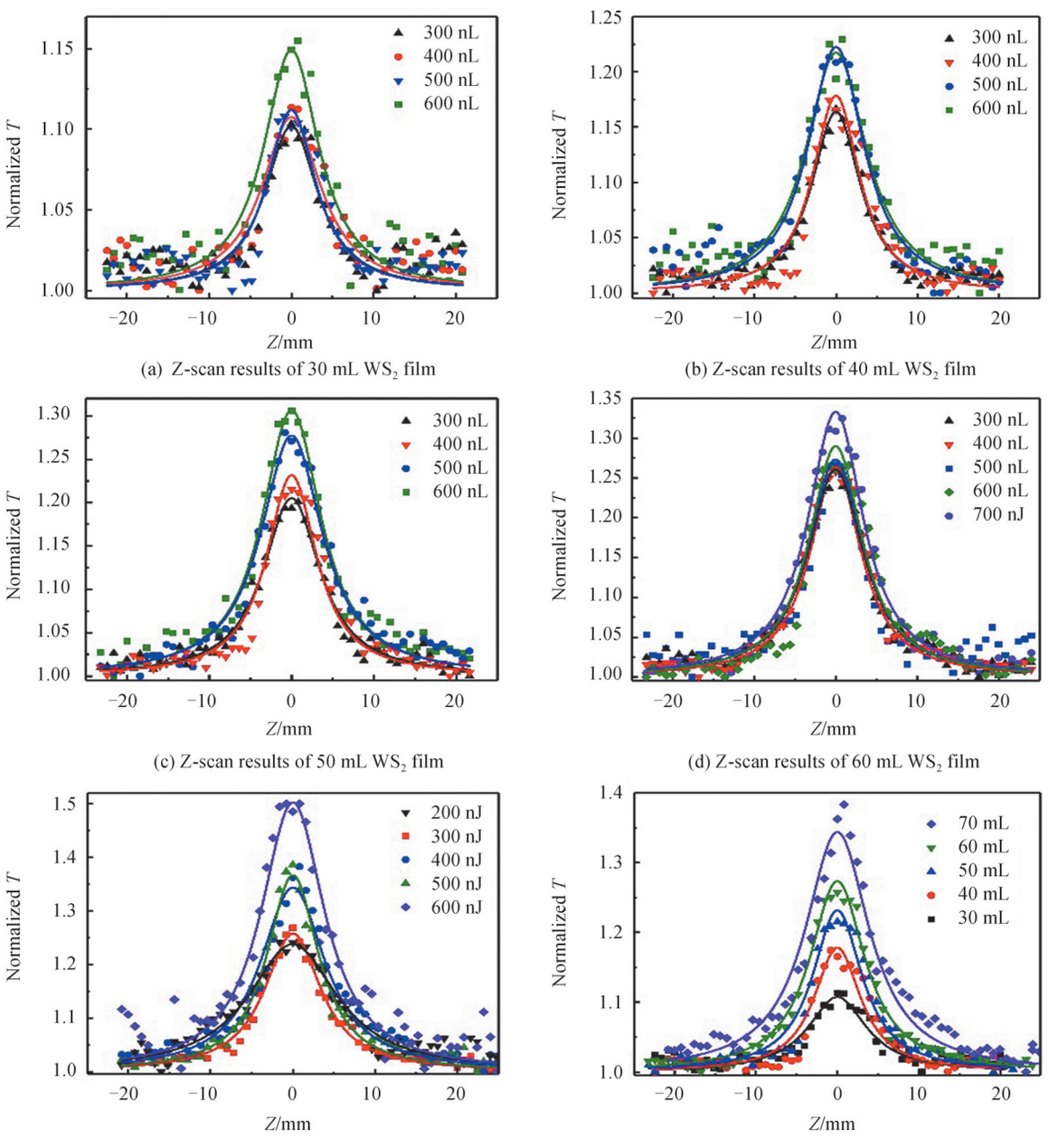

(a) Z-scan results of 30 mL WS_2 film
(b) Z-scan results of 40 mL WS_2 film
(c) Z-scan results of 50 mL WS_2 film
(d) Z-scan results of 60 mL WS_2 film
(e) Z-scan results of 70 mL WS_2 film
(f) Z-scan results of 30~70 mL WS_2 films

图2　不同抽滤体积下的Z扫描结果

Fig. 2　Z-scan results of WS_2 films with different filtration volumes

子吸收饱和所引起的。为了进一步研究不同厚度薄膜的非线性吸收特性，选取同一入射泵浦能量(400 nJ)下的Z扫描结果，研究发现随着厚度增加，焦点处(Z=0)透射率变大。为了比较不同厚度的饱和吸收是否有变化，采用式(1)～(2)进行拟合计算[15]。在此考虑低能量激发机制，样品的吸收系数可表示为

$$\alpha(I)=\alpha_0+\alpha_{\mathrm{NL}}(I) \tag{1}$$

通过归一化透过率曲线计算可得到非线性吸收系数

$$T_{\mathrm{norm}}=\sum_{m=0}^{\infty}\frac{\left[-\alpha_{\mathrm{NL}}I_0L_{\mathrm{eff}}/(1+z^2/z_0{}^2)\right]^m}{(m+1)^{3/2}}\quad(m=1,2,3) \tag{2}$$

式中，T_{norm}和z_0分别为归一化透射率以及高斯光束的瑞利长度。I、Z和α_{NL}分别为入射光强、样品的传输距离以及非线性吸收率。$L_{\mathrm{eff}}=(1-\mathrm{e}^{-\alpha_0 L})/\alpha_0$为样品的有效厚度，其中，$L$和$I_0$为样品厚度以及焦点处光强。$\alpha_0$可以根据朗达-比尔定律，通过可见-紫外吸收光谱得到。计算的样品线性吸收率(α_0)分别为1.7×10^4 cm^{-1}，1.87×10^4 cm^{-1}，2.14×10^4 cm^{-1}，2.26×10^4 cm^{-1}，2.20×10^4 cm^{-1}，如图3(a)所示。

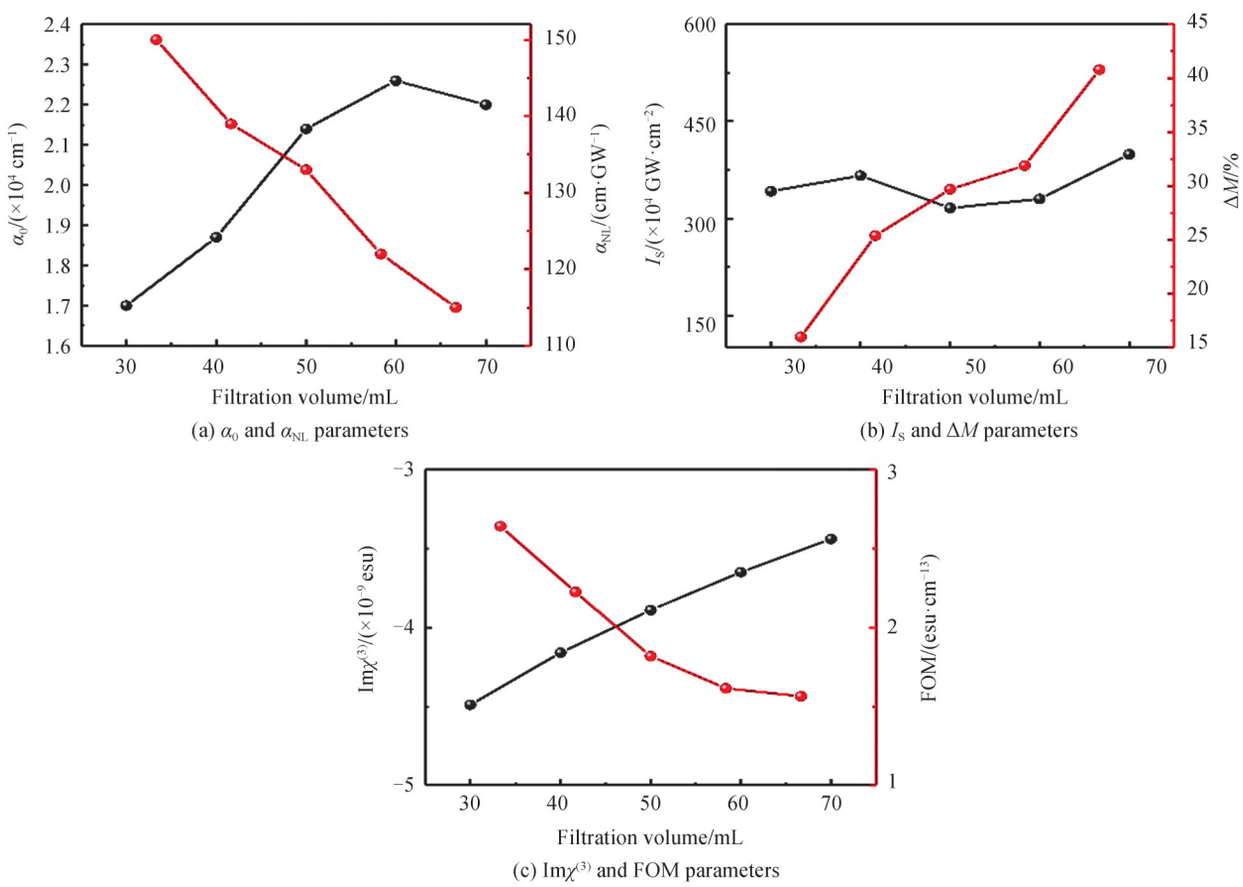

图3 不同抽滤体积下的WS_2非线性参数计算结果

Fig. 3 The calculated nonlinear optical parameters of WS_2 films with different filtration volumes

根据式(1)～(2)，通过计算得到30 mL的WS_2的α_{NL}约为－150 cm/GW，在同等条件下得到40 mL的WS_2(α_{NL}～－139 cm/GW)，50 mL的WS_2(α_{NL}～－133 cm/GW)，60 mL的WS_2(α_{NL}～－122 cm/GW)，70 mL的WS_2(α_{NL}～－115 cm/GW)。结果表明WS_2具有厚度依赖的非线性吸收，这与传统晶体材料的非线性现象不一致，这可能与样品自吸收效应[16]以及表面缺陷有关[17]。本文样品中样品的荧光效率较低，可以排除自吸收效应的影响。从图3(a)中，观察到线性吸收随厚度的增加而增加，这个结果与缺陷态的不断增加有关。较厚的样品缺陷态的增加主要是由于制备的纳米片中的缺陷也会随着层与层的堆叠相应的增加。这种缺陷态的存在会引起更多的非线性散射和能量损失，从而降低非线性吸收[17]。一定的缺陷的存在会引入缺陷能级，更有利于在红外和近红外的调Q和锁模激光器中的应用。同时饱和光强(I_S)和调制深度(ΔM)也是评价饱和吸收体的重要的性能参数，可以通过式(3)得到。

$$T=1-\frac{\Delta M\times I_S}{I_S+I_0/(1+\frac{Z^2}{Z_0{}^2})}/(1-\Delta M) \tag{3}$$

随着抽滤体积的增加，通过式(3)计算的饱和光强依次为342 GW/cm^2，366 GW/cm^2，316 GW/cm^2，330 GW/cm^2，399 GW/cm^2，调制深度分别为16%，25.4%，29.7%，31.9%，40.8%，如图3(b)。随着厚度的增加，调制深度增大主要来源于材料的吸收增加。较高的调制深度以及相对较低的饱和光强证实WS_2可以作为饱和吸收体应用到光子学器件中[18]。为了进一步分析样品的三阶非线性极化率虚部($\mathrm{Im}\,\chi^{(3)}$)，利用式(4)进行计算。

$$\mathrm{Im}\,\chi^{(3)}(\mathrm{esu})=\left[\frac{10^{-7}c\lambda n^2}{96\pi^2}\right]\alpha_{\mathrm{NL}} \tag{4}$$

如图3(c)所示，得到的抽滤体积为30 mL的WS_2的$\mathrm{Im}\,\chi^{(3)}$约为-4.49×10^{-9} esu，在同等条件下得到抽滤体积40 mL的WS_2($\mathrm{Im}\,\chi^{(3)}\sim-4.16\times10^{-9}$ esu)，50 mL的WS_2($\mathrm{Im}\,\chi^{(3)}\sim-3.89\times10^{-9}$ esu)，60 mL的WS_2($\mathrm{Im}\,\chi^{(3)}\sim-3.65\times10^{-9}$ esu)，70 mL的WS_2($\mathrm{Im}\,\chi^{(3)}\sim-3.44\times10^{-9}$ esu)。进一步，薄膜的品质因子(Figure of Merit，FOM)，可以从式(5)得到。

$$\mathrm{FOM}=\left|\mathrm{Im}\,\chi^{(3)}/\alpha_0\right| \tag{5}$$

如图3(c)所示，计算得到体积为30 mL的WS_2的FOM约为2.64×10^{-13} esu·cm，在同等条件下得到体积40 mL的WS_2(FOM$\sim2.22\times10^{-13}$ esu·cm)，50 mL的WS_2(FOM$\sim1.81\times10^{-13}$ esu·cm)，60 mL的WS_2(FOM$\sim1.61\times10^{-13}$ esu·cm)，70 mL的WS_2(FOM$\sim1.56\times10^{-13}$ esu·cm)。结果表明30 mL制备的WS_2样品更适合应用到光子学器件当中。

2.1 机理分析

由于多层WS_2的带隙接近于块体材料，为了进一步理解WS_2的可饱和吸收特性，使用密度泛函理论利用VASP软件计算得到了块体WS_2的能带。图4(a)是WS_2的能带结构，证实WS_2是间接带隙半导体。在价带顶和导带底之间主要有两种跃迁方式，一种是跃迁能量为1.6 eV的K→K直接跃迁，另一种以及能量为0.8 eV的Γ→Γ－K间接跃迁[19]。根据吸收理论，当一个能量为1.55 eV的光子入射到WS_2薄膜时，处于价带中的电子将会被激发到导带上，如图4(b)所示。由于WS_2能带的间接跃迁方式，电子将从价带中吸收光子激发到导带中。激发的电子占据导带中的低能量状态。随着入射能量的增加，导带内的量子态被激发的电子填满[20]。根据泡利不相容原理，两个电子不能占据相同量子态，造成光子不再被吸收从而使得透射光不断增加，此时WS_2达到饱和。

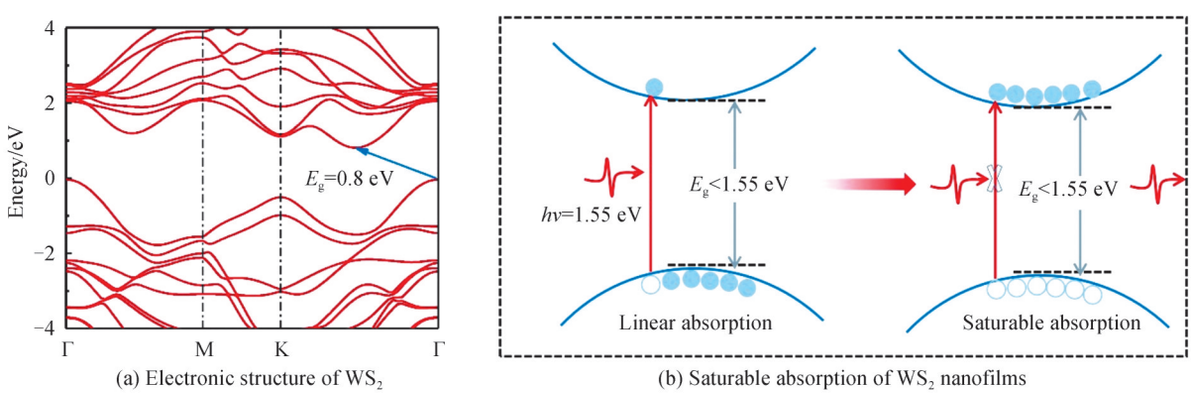

图4 WS_2样品的饱和吸收过程

Fig. 4 The process of saturable absorption of WS_2 nanofilms

3 结论

本文利用液相剥离方法获得了分散均匀的WS_2纳米片，通过控制抽滤体积成功制备了大面积不同厚度的薄膜。Z扫描结果显示不同厚度的WS_2均表现出可饱和吸收的特性，这主要源自于带隙填充的泡利阻塞

效应。随着厚度的增加，饱和强度基本不变，调制深度会提高，主要源自于样品的吸收随着厚度的增加而增强。三阶非线性极化率的虚部的绝对值和品质因子随着厚度的增加而降低，主要归因于较厚样品的较多的缺陷态使得捕获光生载流子的能力增强。大面积制备的WS_2薄膜可作为可饱和吸收体应用于调Q激光器以及锁模激光器，为设计可用于高性能超快开关和超快激光的二维材料提供了参考。

参考文献

[1] MALDONADO M E, DAS A, JAWAID A M, et al. Nonlinear optical interactions and relaxation in 2D layered transition metal dichalcogenides probed by optical and photoacoustic Z-scan methods[J]. ACS Photonics, 2020, 7(12): 3440-3447.

[2] CHANG Yunghuang, ZHANG Wenjing, ZHU Yihan, et al. Monolayer $MoSe_2$ grown by chemical vapor deposition for fast photodetection[J]. ACS Nano, 2014, 8(8): 8582-8590.

[3] YANG Weihuang, SHANG Jingzhi, WANG Jianpu, et al. Electrically tunable Valley-Light Emitting Diode (vLED) based on CVD-grown monolayer WS_2[J]. Nano Letters, 2016, 16(3): 1560-1567.

[4] JARIWALA D, SANGWAN V K, LAUHON L J, et al. Emerging device applications for semiconducting twodimensional transition metal dichalcogenides[J]. ACS Nano, 2014, 8(2): 1102-1120.

[5] HUANG Yuanyuan, ZHU Lipeng, ZHAO Qiyi, et al. Surface optical rectification from layered MoS_2 crystal by THz timedomain surface emission spectroscopy[J]. ACS Applied Materials & Interfaces, 2017, 9(5): 4956-4965.

[6] E Yiwen, ZHANG Liangliang, TCYPKIN A, et al. Broadband THz sources from gases to liquids[J]. Ultrafast Science, 2021, 2021: 9892763.

[7] PESCI F M., SOKOLIKOVA M S, GROTTA C, et al. MoS_2/WS_2 heterojunction for photoelectrochemical water oxidation[J]. ACS Catalysis, 2017, 7(8): 4990-4998.

[8] WANG Gaozhong, BAKER M A A, BLAU W J. Saturable absorption in 2D nanomaterials and related photonic devices [J]. Laser & Photonics Reviews, 2019, 13(7): 1800282.

[9] DONG Ningning, LI Yuanxin, FENG Yanyan, et al. Optical limiting and theoretical modelling of layered transition metal dichalcogenide nanosheets[J]. Scientific Reports, 2015, 5(1): 14646.

[10] ZHOU Kaige, ZHAO Min, CHANG Mengjie, et al. Size-dependent nonlinear optical properties of atomically thin transition metal dichalcogenide nanosheets[J]. Small, 2015, 11(6): 694-701.

[11] LU Chunhui, YANG Dan, MA Jingyao, et al. Effect of surface oxidation on nonlinear optical absorption in WS_2 nanosheets[J]. Applied Surface Science, 2020, 532: 147409.

[12] LU Chunhui, MA Jingyao, SI Keyu, et al. Band alignment of WS_2/MoS_2 photoanodes with efficient photoelectric responses based on mixed van der waals heterostructures[J]. Physica Status Solidi, 2019, 216(20): 1900544.

[13] LU Chunhui, XUAN Hongwen, ZHOU Yixuan, et al. Saturable and reverse saturable absorption in molybdenum disulfide dispersion and film by defect engineering[J]. Photonics Research, 2020, 8(9): 1512-1521.

[14] QUAN Chenjing, LU Chunhui, HE Chuan, et al. Band alignment of $MoTe_2/MoS_2$ nanocomposite films for enhanced nonlinear optical performance[J]. Advanced Materials Interfaces, 2019, 6(5): 1801733.

[15] QUAN Chenjing, HE Minmin, HE Chuan, et al. Transition from saturable absorption to reverse saturable absorption in $MoTe_2$ nano-films with thickness and pump intensity[J]. Applied Surface Science, 2018, 457: 115-120.

[16] LIU Dong, LIU Junting, ZHANG Kangning, et al. Giant nonlinear optical response of lead-free all-inorganic $CsSnBr_3$ nanoplates[J]. The Journal of Physical Chemistry C, 2021, 125(1): 803-811.

[17] ZHANG Jun, JIANG Tian, ZHENG Xin, et al. Thickness-dependent nonlinear optical properties of $CsPbBr_3$ perovskite nanosheets[J]. Optics Letters, 2017, 42(17): 3371-3374.

[18] ZHANG Baitao, LIU Jun, WANG Cong, et al. Recent progress in 2D material-based saturable absorbers for all solid-state pulsed bulk lasers[J]. Laser & Photonics Reviews, 2019, 14(2): 1900240.

[19] ZHANG Longhui, HUANG Yuanyuan, ZHAO Qiyi, et al. Terahertz surface emission of d-band electrons from a layered tungsten disulfide crystal by the surface field[J]. Physical Review B, 2017, 96(15): 155202.

[20] CHEN Runze, ZHENG Xin, JIANG Tian. Broadband ultrafast nonlinear absorption and ultra-long exciton relaxation time of black phosphorus quantum dots[J]. Optics Express, 2017, 25(7): 7507-7519.

Thickness-dependent Third-order Nonlinear Optical Absorption of WS_2 Nanofilms

JIN Yanping[1], LU Chunhui[1], ZHAO Qiyi[2], XU Xinlong[1]
(1 *School of Physics, Northwest University, Xi'an* 710127, *China*)
(2 *School of Science, Xi'an University of Posts & Telecommunications, Xi'an* 710121, *China*)

Abstract: Two-dimensional (2D) layered materials with excellent properties such as strong spin-valley coupling, high current on/off ratio and carrier mobility, have gained great attentions in optoelectronic applications including photodetectors, field effect transistors and light-emitting diodes. Meanwhile, many Novel Nonlinear Optical (NLO) phenomena such as saturable absorption, reverse saturable absorption and two-photon absorption have also been observed. Based on these nonlinear absorption behaviors, ultrafast photonic applications including Q-switching, mode locking and optical limiting have successfully been designed in 2D materials. The device performance is strongly dependent on their thicknesses due to tunable electronic properties with layer. For example, giant two-photon absorption can be observed in monolayer WS_2 film with 1.9 eV while excellent saturable absorption has been demonstrated in multilayer. However, the related research about NLO nonparametric processes with layer thickness, which is crucial to design high performance photonic devices, was seldom reported due to uncontrollable thickness in large-area. Therefore, seeking for an efficient way to produce large-scale and controllable film is highly desirable. To date, mechanical exfoliation have been developed to acquire few-layer nanosheet through exfoliating bulk material layer by layer. However, these methods are low reproducibility and low yield and even limit their application in photonic devices. Compared with mechanical exfoliation method, liquid phase exfoliation was quickly developed and most 2D materials were successfully exfoliated to few-layer or monolayer nanosheet. The nanosheet dispersion can be used to form wafer-scale film by vacuum filtration technique, which provides an effective way to prepare large-area film. Herein, WS_2 nanosheet dispersion was prepared by liquid phase exfoliation and then WS_2 films with different thicknesses were prepared by a vacuum filtration method with different volumes. The atomic force microscopy confirmed the nanosheet length is between 2 and 4 μm and the thickness of thin film is 50 nm for 30 mL in fltration volumes. Raman spectroscopy was used to charaterize the sample composition and the typical Raman peaks confirmed the preparation of WS_2 films. UV-Vis spectra was used to obtain the linear absorption and vetified the defects in the grain boundary. The third-order NLO absorption of prepared WS_2 nanofilms was studied by a Z-scan technique based on 800 nm femtosecond laser. It is found that all WS_2 with different thicknesses show the characteristics of saturable absorption, which is mainly due to the Pauli blocking effect caused by single photon absorption. To confirm the absorption process, the electronic structure was calculated by density functional theory and the calculated bandgap of bulk WS_2 is approximately 0.8 eV. The photon energy is higher than the bandgap, which vertified the single photon absorption occurs. The nonlinear absorption coefficients are −150 cm/GW, −139 cm/GW, −133 cm/GW, −122 cm/GW, and −115 cm/GW from 30 mL to 70 mL fltration volumes. Obviously, the absolute value of nonlinear absorption coefficients decreases with the incereased thickness. This decrease is mainly due to the reason that thicker films with high density defects capture more photoexcited carriers and generate more nonlinear scattering as well as energe loss, resulting in the dependence of third-order nonlinear optical absorption with thicknesses. The existence of certain defects will introduce defect energy levels, which has a great potential in the application of infrared and near-infrared Q-switched and mode-locked lasers. With the increase of thickness, the saturation intensity is basically unchanged, and the modulation depth increases while the absolute values of the imaginary part of the third-order nonlinear optical susceptibility and figure of merit decrease. Our results provide provide experimental support for the applications of WS_2 thin films in ultrafast switchers and ultrafast lasers.

Key words: Tungsten disulfide (WS_2); Third order optical nonlinearity; Saturable absorption; Thickness dependence; Z-scan
OCIS Codes: 160.4330; 230.0250

Foundation item: National Natural Science Foundation of China (Nos. 11774288, 12074311), Natural Science Foundation of Shannxi Province, China (No. 2019-JC25)